

## Dynamics in the DNA Recognition by DAPI: Exploration of the Various Binding Modes

Debapriya Banerjee and Samir Kumar Pal\*

Unit for Nano Science & Technology, Department of Chemical, Biological & Macromolecular Sciences, S. N. Bose National Centre for Basic Sciences, Block JD, Sector III, Salt Lake, Kolkata 700 098, India

Received: September 4, 2007; In Final Form: October 22, 2007

Two distinct modes of interaction of the fluorescent probe 4',6-diamidino-2-phenylindole (DAPI), depending on the sequence of DNA, have been reported in the literature. In the present study, the dynamics of solvation has been utilized to explore the binding interaction of DAPI to DNA oligomers of different sequences. Picosecond-resolved fluorescence and polarization-gated anisotropy have been used to characterize the binding of DAPI to the different oligomers. In the double-stranded dodecamer of sequence CGCGAATTCGCG (oligo1), the solvation relaxation dynamics of the probe reveals time constants of 0.130 ns (75%) and 2.35 ns (25%). Independent exploration of the minor-groove environment of oligo1 using another well-known minor-groove binder Hoechst 33258 (H258) shows similar timescales, further confirming minor-groove binding of DAPI to oligo1. In the double-stranded dodecamer (oligo2) having the sequence GCGCGCGCGCGC, where intercalation has been reported in the literature, no solvation is observed in our experimental window. DAPI bound to oligo2 shows quenching of fluorescence compared to that of DAPI in a buffer. The quenching of fluorescence of DAPI intercalated in DNA is also borne out by the appearance of a fast component of 30 ps in the fluorescence lifetime, revealing electron transfer to DAPI from GC base pairs, between which it intercalates. In addition to this, the excited-state lifetime of the probe in the DAPI–DNA complex also shows a time constant similar to that of the dye in a buffer, indicating that the excited-state photoprocesses associated with the free dye is also operative in this binding mode, consistent with the binding geometry of the DAPI in the DNA. The dynamics of DAPI in calf thymus DNA having a random sequence of base pairs is similar to that associated with the DNA minor groove. Our studies clearly explore the structure–dynamics correlation of the DAPI–DNA complex in the two distinct modes of interaction of DAPI with DNA.

### Introduction

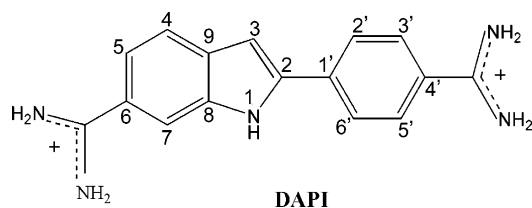
The fluorescent probe 4',6-diamidino-2-phenylindole (DAPI) is an efficient DNA binder.<sup>1</sup> Studies on DAPI–DNA complexes have shown that DAPI exhibits a wide array of interaction of varying strength and specificity with DNA.<sup>1–14</sup> The binding of DAPI to DNA is strongly dependent on the DNA sequence.<sup>7–9,11,12</sup> Complexes with DAPI bound in the minor groove,<sup>1,10</sup> major groove,<sup>3</sup> and by intercalation<sup>2,6,14</sup> have been proposed on the basis of a variety of experimental observations with DNA having different sequences. The X-ray crystal structure of DAPI bound to a DNA oligomer<sup>1</sup> having the sequence CGCGAATTCGCG shows that the dye binds to the minor groove in the central AATT region. It has been suggested that the minor-groove binding of DAPI requires the presence of four consecutive AT/TA sequence. However, a study<sup>4</sup> has shown that in a decamer having the sequence CGCGAATTCG, the probe shows off-centered minor-groove binding. In DNA oligomer sequences having no consecutive AT base pairs or having GC base pairs only, it has been suggested that DAPI intercalates between the GC base pairs.<sup>2,6,14</sup> The intercalative binding mode of DAPI to DNA is also controversial, and many workers have suggested alternative binding modes like electrostatic attraction<sup>5</sup> and major-groove binding<sup>3</sup> for DAPI in GC DNA. In addition to the above-mentioned modes of binding to DNA, several unique binding modes like  $\pi$ – $\pi$  stacking interactions,<sup>9</sup> nonclassical intercalation,<sup>12</sup> and allosteric binding<sup>13</sup> of DAPI to DNA have also been reported. It is to be noted that over the years, the dynamics of

solvation has evolved as an efficient technique to explore the binding interactions of ligands with biological macromolecules like DNA and proteins.<sup>15–22</sup> Although a variety of techniques like X-ray crystallography, NMR, DNase footprinting, circular dichroism, and electric linear dichroism techniques have been employed to study DAPI–DNA interactions, to date, solvation studies have not been used to explore the binding of DAPI to different DNA sequences.

Characterization of the binding of DAPI to two double-stranded DNA dodecamers having the sequences CGCGAATTCGCG (oligo1) and GCGCGCGCGCGC (oligo2) by using the dynamics of solvation reported by the probe is the motivation of this study. The efficacy of DAPI to report the dynamics of solvation in restricted environments like biomimetics has been established in a separate study (to be published elsewhere). The time-resolved data have been acquired by a picosecond-resolved time-correlated single-photon counting technique (TCSPC). Picosecond-resolved fluorescence and polarization-gated anisotropy have been used to characterize the rigidity of the probe environments in the DAPI–DNA complexes. A parallel investigation of the environmental dynamics of the minor groove of oligo1 is carried out with the well-known minor-groove binder Hoechst 33258 (H258). Our experimental observations show a slow solvation characteristic of minor-groove binding in the DAPI–oligo1 complex, whereas in oligo2 there is no solvation in our experimental time window in accordance with an intercalative binding mode. The environmental dynamics of calf thymus DNA of random sequence is also reported for comparison.

\* Corresponding author. Fax: 91 33 2335 3477. E-mail: skpal@bose.res.in.

### SCHEME 1: Schematic Representation of the Probe DAPI



### Materials and Methods

Calf thymus (CT) DNA and phosphate buffer were obtained from Sigma. The probes DAPI (Scheme 1) and Hoechst 33258 (H258) were obtained from Molecular Probes. The DNA oligomers having sequences CGCGAATTCGCG (oligo1) and GCGCGCGCGCGC (oligo2) were obtained from GeneLink (USA), purified by Reverse Phase Cartridge (RPC) technique, and checked by gel electrophoresis. The gel electrophoresis result indicated a single spot consistent with pure dodecamer DNA. All the solutions were prepared in 50 mM phosphate buffer (pH = 7.0) using water from the Millipore system. The oligomers were dialyzed in phosphate buffer for 4 h for further use. The probe–DNA (oligo1, oligo2, and CT DNA) solutions were prepared by adding the requisite amount of probe stock solution (prepared in water) to DNA and stirring for 1 h. To ensure complete complexation of the probe with the DNAs, the probe concentration was much less (1  $\mu$ M) than that of the DNAs ([oligo1] = 6  $\mu$ M, [oligo2] = 6  $\mu$ M, and [CT DNA] = 100  $\mu$ M (base pairs)]. The melting points of oligo1 and oligo2 are reported to be 40 and 48  $^{\circ}$ C, respectively. To ensure that oligo1 and oligo2 are in their double-stranded form, the experiments are done at 20  $^{\circ}$ C.

Steady-state absorption and emission are measured with a Shimadzu UV-2450 spectrophotometer and a Jobin Yvon Fluoromax-3 fluorimeter, respectively. Fluorescence transients are measured and have been fitted by using a commercially available spectrophotometer (LifeSpec-ps) from Edinburgh Instrument, U.K. (excitation wavelength 375 nm, 80 ps instrument response function (IRF)). The quality of the curve fitting is evaluated by reduced  $\chi$ -square and residual data. The Time-Resolved Emission Spectra (TRES) and the Time-Resolved Area Normalized Spectra (TRANES) are constructed according to the methodologies described in our previous studies.<sup>23,24</sup> The solvation correlation function,  $C(t)$  is constructed according to the following the equation:

$$C(t) = \frac{\nu(t) - \nu(\infty)}{\nu(0) - \nu(\infty)} \quad (1)$$

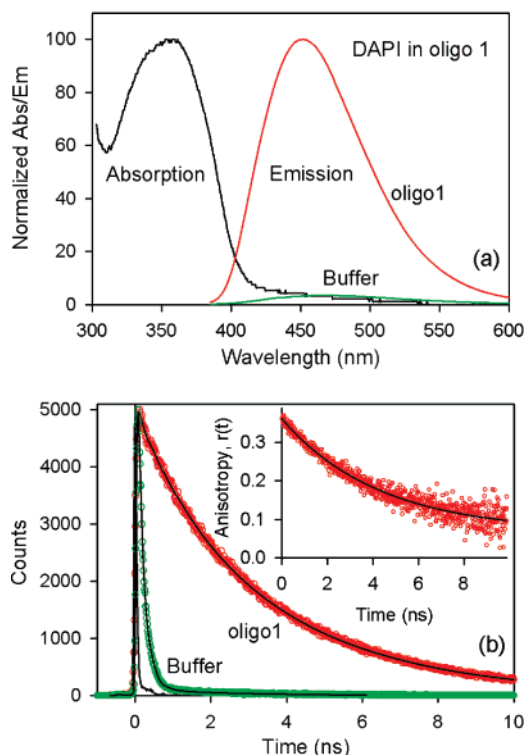
where  $\nu(0)$ ,  $\nu(t)$ , and  $\nu(\infty)$  stand for the wavenumber in  $\text{cm}^{-1}$  at the emission maxima at time zero,  $t$ , and infinity, respectively. For anisotropy ( $r(t)$ ) measurements, emission polarization is adjusted to be parallel or perpendicular to that of the excitation and anisotropy is defined as

$$r(t) = \frac{[I_{\text{para}} - GI_{\text{perp}}]}{[I_{\text{para}} + 2GI_{\text{perp}}]} \quad (2)$$

where  $G$ , the grating factor, is determined following the long-time tail-matching technique<sup>25</sup> to be 1.2.

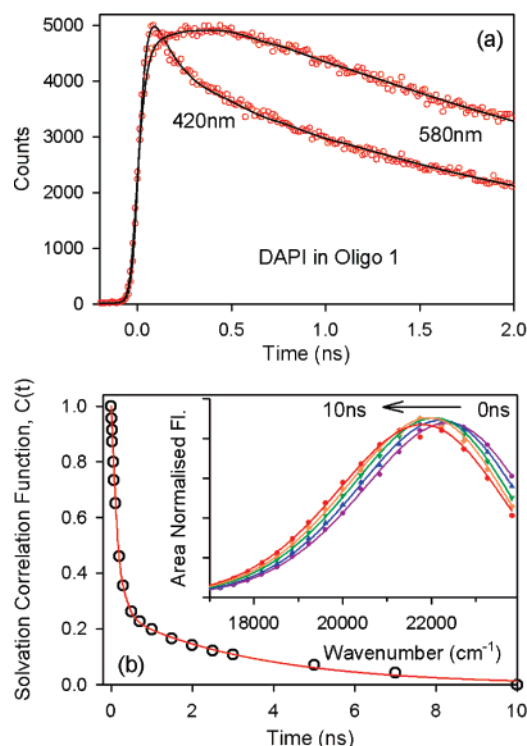
### Results and Discussion

Figure 1a shows absorption and emission spectra of DAPI bound to oligo1. The absorption spectrum shows a red-shift



**Figure 1.** The absorption and emission spectra (a), the temporal decay of fluorescence (b), and fluorescence anisotropy (inset) of DAPI ([DAPI] = 1  $\mu$ M) bound to the double-stranded dodecamer of sequence CGCGAATTCGCG (oligo1) ([oligo1] = 6  $\mu$ M). The emission spectrum (a) and the temporal decay of fluorescence (b) of DAPI in buffer (50 mM phosphate buffer pH = 7) are shown for comparison (green). The instrument response function IRF is also shown in black (b).

compared to that of the probe in buffer, consistent with the ground-state stabilization of a positively charged probe in negatively charged DNA. The emission spectrum shows a blue-shift, compared to the emission in bulk buffer, suggesting that the excited-state dipole of the probe is less stabilized in the less polar and hydrophobic DNA environment. In this regard, it should be noted that although bound waters hydrate the DNA minor groove, the polarity of the minor groove is less than that of water.<sup>26</sup> The probe also shows a significant (28 times) increase in the fluorescence intensity when bound to oligo1 compared to that of DAPI in bulk buffer. The increase of fluorescence is consistent with the high affinity binding in the minor groove, as reported in other studies.<sup>8</sup> The X-ray crystal structure<sup>1</sup> of DAPI bound to the oligomer of the same sequence shows that the probe inserts itself edgewise into the narrow minor groove, displacing the ordered spine of hydration. In this mode of binding, DAPI and a single water molecule together span the four AT base pairs present at the center of the duplex. The indole nitrogen of the probe (Scheme 1) forms a bifurcated hydrogen bond with the thymine oxygen atoms of the two central base pairs, as with netropsin and Hoechst 33258 (H258). Figure 1b shows the temporal decay of fluorescence of the DAPI–oligo1 complex and that of free DAPI in buffer. The time constants associated with the decay of DAPI in the DAPI–oligo1 complex are in the order of nanoseconds, compared to the fast decay of the probe (100 ps), in bulk buffer. The inset of Figure 1b shows the temporal decay of fluorescence anisotropy of the DAPI–oligo1 complex. The time constant associated with the decay is 4.5 ns. The observed time constant is in close agreement with the value of 4.6 ns reported by H258 in the minor groove of the same DNA oligomer (see below). It is to be noted that the time constant associated with the decay of



**Figure 2.** The fluorescence transients (a), the solvation correlation function (b), and TRANES (inset of b) of DAPI ( $[\text{DAPI}] = 1 \mu\text{M}$ ) bound to the double-stranded dodecamer of sequence CGCGAATTCGCG (oligo1) ( $[\text{oligo1}] = 6 \mu\text{M}$ ).

rotational anisotropy of the probe in aqueous buffer is 100 ps. The absence of any subnanosecond component in the decay of fluorescence anisotropy in oligo1 shows that DAPI fits tightly into the minor groove of oligo1.

To construct the time-resolved emission spectrum (TRES), the fluorescence transients are taken at the blue and red ends of the emission spectrum (Figure 2a). The transients show fast decay in the blue end and rise in the red end indicative of solvation.<sup>17</sup> The constructed TRES show a spectral shift of  $700 \text{ cm}^{-1}$  in a 10 ns window. To ascertain whether the associated spectral shift is due to the environmental relaxation or is associated with some intramolecular photoprocesses, (e.g., formation of excited-state species) the time-resolved area normalized emission spectra (TRANES) are constructed. The TRANES technique is widely used to determine the kind of species present in the system and the environment around the species.<sup>23,24</sup> A useful feature of the method is that an isoemissive point in the spectra involves two emitting species, which are kinetically coupled either irreversibly or reversibly or not coupled at all. In recent literature, various other studies have also used the TRANES technique to confirm different emissive species in micro-heterogeneous environments.<sup>23,24</sup> The inset of Figure 2b shows the constructed TRANES. The absence of isoemissive points in the TRANES shows that a single conformer is involved in the relaxation process, and the process indeed reflects environmental stabilization. The solvation correlation function (Figure 2b) decays with time constants of 130 ps (75%) and 2.35 ns (25%), which reflect the environmental relaxation of the minor groove of oligo1.

It is known that the dynamics of solvation represents the environmental stabilization of the excited state of a probe. The environmental stabilization is independent of the nature of the probe molecule. In order to obtain a general picture of the environmental dynamics of the minor groove, we have used

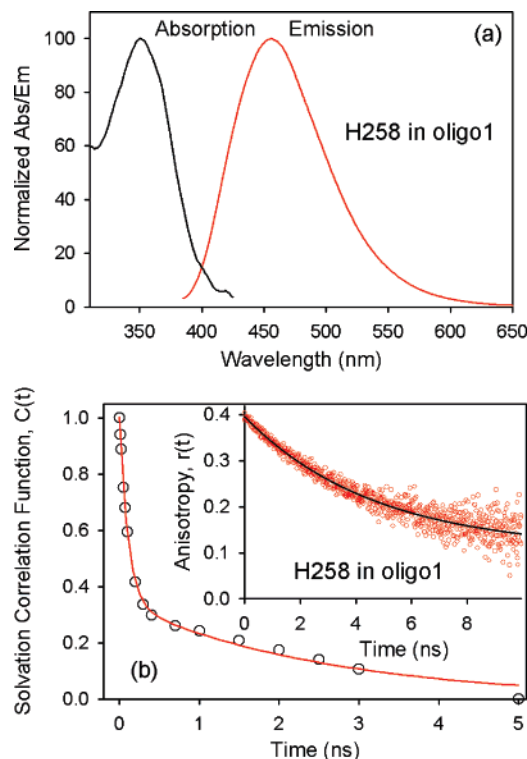


**Figure 3.** The absorption and emission spectra (a), and temporal decay of fluorescence anisotropy (inset of b) and solvation correlation function (b) of H258 ( $[\text{H258}] = 1 \mu\text{M}$ ) bound to oligo1 ( $[\text{oligo1}] = 6 \mu\text{M}$ ).

the well-known minor-groove binder H258 to independently probe the dynamics of the minor groove of oligo1. The binding of H258 to oligo1 has been confirmed from X-ray crystallographic studies.<sup>27</sup> Figure 3a shows the absorption and emission spectra of H258 in oligo1. The red-shift in the absorption spectrum and blue-shift in the emission spectrum of the H258–oligo1 complex, compared to that of H258 in a buffer<sup>28</sup> indicate the binding of the probe to DNA. The time constant of 4.6 ns in the temporal decay of fluorescence anisotropy (inset of Figure 3b) depicts the overall tumbling motion of oligo1. The absence of any subnanosecond component indicates that the probe motion (500 ps in aqueous buffer<sup>28</sup>) is frozen in the H258–oligo1 complex. The solvation correlation function (Figure 3b) decays with time constants of 110 ps (68%) and 2.58 ns (32%). The striking similarity of the time constants associated with environmental stabilization reported by H258 and DAPI clearly shows that both the probes occupy the minor groove of oligo1. Thus, the dynamics of solvation provides direct evidence of the minor-groove binding of DAPI.

Figure 4a shows the absorption and emission spectra of DAPI bound to oligo2. As observed earlier with oligo1, the absorption spectrum is red-shifted and the emission spectrum is blue-shifted compared to that of DAPI in bulk buffer. It is to be noted that the probe in oligo2 shows a much-quenched (2 times) fluorescence compared to that of the probe in bulk buffer. According to the existing literature,<sup>8</sup> this is consistent with the low-affinity intercalative binding mode of the probe to DNA sequences where there are no/nonconsecutive AT regions. The quenching of fluorescence suggests that there is an additional mode of excited-state relaxation of DAPI in the DAPI–oligo2 complex, compared to that in a buffer. It is known from *ab initio* studies<sup>29</sup> that DAPI is a good electron acceptor and DNA bases, especially guanine, are good electron donors. So electron transfer from DNA bases to DAPI could be a possible mode of excited-state

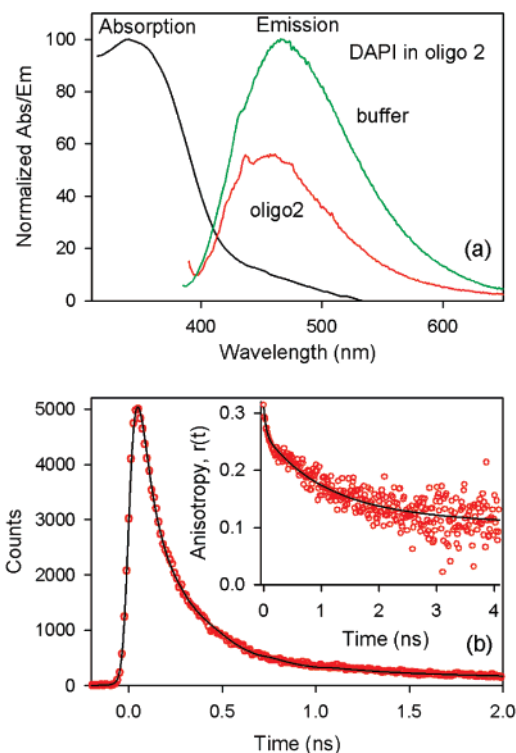


**Figure 4.** The absorption and emission spectra (a), the temporal decay of fluorescence (b), and fluorescence anisotropy (inset of (b)) of DAPI ([DAPI] = 1  $\mu$ M) bound to the double-stranded dodecamer of sequence GCGCGCGCGCGC (oligo2) ([oligo2] = 6  $\mu$ M). The emission spectrum of DAPI in 50 mM phosphate buffer (green) is shown for comparison.

relaxation. The electron-transfer process is also evident from the appearance of an additional fast component of 30 ps (40%) in the temporal decay of fluorescence of DAPI in oligo2 (Figure 4b). This component is faster than that associated with the free probe in a buffer (130 ps) and is indicative of the fast electron transfer from DNA to DAPI. In addition to this 30 ps component, DAPI shows another component of 150 ps, similar to that of DAPI in a buffer. The similarity of the relatively slower time constants of 150 ps associated with the fluorescence decay of the probe in the GC dodecamer (oligo2) and buffer is in accordance with a previously reported study,<sup>5</sup> where it has been interpreted as a nonintercalative electrostatic binding of DAPI to GC DNA. However, perhaps due to limited resolution (phase correlation technique), the faster component of 30 ps has not been reported in the aforesaid study. The 150 ps component in the excited-state relaxation of DAPI in the DAPI–oligo2 complex is associated with proton transfer (proton transfer of DAPI in buffer is known from earlier studies<sup>30,31</sup>). This shows that both intramolecular proton transfer and electron transfer from the DNA base to DAPI are associated with the excited-state relaxation of DAPI in the DAPI–oligo2 complex. Since the proton transfer in DAPI is intramolecular, it involves the redistribution of positive charge density in the molecule itself, hence, concomitant electron transfer can also occur. Concerted electron transfer and proton-transfer processes are reported in the literature.<sup>32,33</sup> The temporal decay of fluorescence anisotropy of DAPI in oligo2 (inset of Figure 4b) also shows a fast component of 40 ps (20%) indicative of the electron transfer. The additional time components of 1.3 ns (55%) and 6 ns (25%) associated with the decay of fluorescence anisotropy indicate restricted motions of the probe and the overall tumbling motion of DNA, respectively.<sup>34</sup> The observation of electron transfer

from DNA base pairs to DAPI in the DAPI–oligo2 complex gives further support to the intercalative binding mode in the DAPI–oligo2 complex and rules out the possibility of major-groove binding of DAPI in oligo2. The similarity of the fluorescence transients at the blue and red ends of the spectrum reveals that there is no solvation stabilization in the experimental time window.

To explain the observation of proton transfer for DAPI bound to oligo2, it is essential to have a clear picture of the intercalative binding mode. Molecular modeling studies of DAPI bound to RNA sequence A<sub>3</sub>U<sub>8</sub>, where the dye intercalates, have been used to determine the binding geometry of the probe in the intercalative binding mode.<sup>14</sup> The results show that, in the intercalative binding mode, the indole ring of DAPI is stacked between the adenosines and the phenyl ring of the probe is between uracils. In this binding mode, the DAPI indole–phenyl bond is twisted approximately 8° to match the base pair propeller twist. The amidine groups are rotated 31° with respect to the indole and 32° with respect to the phenyl ring to which they are bound and project out into the major groove in the RNA complex. X-ray analysis with intercalation complexes of dinucleotides and modeling studies with intercalators in the segments of RNA and DNA have indicated that the intercalation sites in both types of nucleic acids are quite similar.<sup>35</sup> This model provides rationalization for the time constants associated with the decay of the fluorescence anisotropy. The 1.3 ns component associated with the decay of fluorescence anisotropy in the DAPI–oligo2 complex reflects the hindered rotation of the amidino groups projected out in the major groove. It is to be noted that the excited-state relaxation of the DAPI in buffer takes place by an intramolecular excited-state proton transfer from the 6-amidino group to the ring<sup>30</sup> through the intervention of the solvation shell surrounding the molecule.<sup>31</sup> In the intercalative binding mode, the amidino groups are projected in the major groove of the oligo2. The average reorientation times of water present in the shallow major groove (average reorientation time = 6 ps) of the DNA are similar to that of free water (average reorientation time = 1 ps).<sup>36</sup> Hence, the proton transfer from the 6-amidino group to the indole ring of DAPI takes place with equal ease. This interpretation rationalizes the observation that a considerable portion of the fluorescence decay of DAPI in GC DNA (oligo2 in the present study) is buffer-like. The absence of solvation in the intercalative binding mode could be due to the fact that the faster solvation, reported for another intercalating dye,<sup>37</sup> is beyond our instrumental resolution.

To render an interesting comparison, the environmental dynamics of the probe has been studied in calf thymus DNA having a random sequence. The absorption spectrum (Figure 5a) of DAPI bound to calf thymus DNA shows a red-shift, similar to the probe–oligo1 complex. The blue-shift and increase in the fluorescence intensity of DAPI when bound to the genomic DNA indicate that the dye resides in a hydrophobic environment. However, the increase in fluorescence intensity is less than that of the probe bound to oligo1. This difference could be attributed to the difference in binding affinity of DAPI to a random DNA sequence. The possibility of DAPI binding to GC regions is less probable because of the stronger binding of DAPI to AT base pairs (binding constant =  $3 \times 10^8$  M<sup>-1</sup>), compared to the binding in GC sequences (binding constant =  $1.2 \times 10^5$  M<sup>-1</sup>).<sup>2</sup> Also, in our study, the concentration of base pairs is 100 times more than that of the probe, ensuring that the probe is bound only in the high-affinity mode. Figure 4a shows the temporal decay of fluorescence intensity of DAPI bound to calf thymus DNA. The time constants associated with

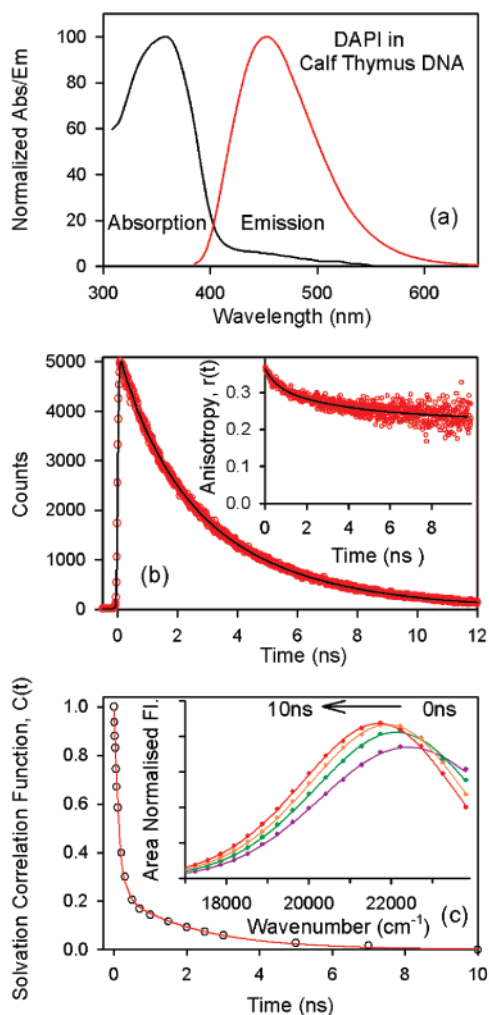


**Figure 5.** The absorption and emission spectra (a), temporal decay of fluorescence (b), fluorescence anisotropy (inset of (b)), the solvation correlation function (c) and TRANES (inset of (c)) of DAPI ([DAPI] = 1  $\mu$ M]) bound to calf thymus DNA ([base pair] = 100  $\mu$ M).

the temporal decay of fluorescence shows nanosecond components similar to that of the probe in oligo1, where DAPI is located in the minor groove of the dodecamer. The temporal decay of fluorescence anisotropy (Figure 5b) shows time constants of 0.652 ns (13%) and 4.47 ns (27%) indicating the restricted motions of the probe and a huge residual indicating the overall tumbling motion of the large DNA. The probe in calf thymus DNA shows a fast decay in the blue end and a rise in the red end indicative of solvation. The constructed TRES shows a spectral shift of 700  $\text{cm}^{-1}$  in a 10 ns window, similar to the DAPI–oligo1 complex. To ascertain whether the observed spectral shift is solely due to solvation stabilization, TRANES (inset of Figure 5c) are constructed for DAPI in calf thymus DNA. The absence of any isoemissive point in the TRANES reveals that the dynamics reports the solvation stabilization of the probe in the DNA environment. The time constants associated with the decay of solvation correlation function are 0.150 ps (74%) and 3.72 ns (24%), similar to that of the probe in oligo1, where the probe is located in the minor groove. The similarity in the dynamical timescales further confirm the groove binding mode in the AT-rich region of calf thymus DNA.

## Conclusion

In the present study, the environmental dynamics of DAPI in double-stranded dodecamers having sequences CGCGAAT-

TCGCG (oligo1) and GCGCGCGCGCGC (oligo2) is explored. The dynamics of the probe in oligo1 shows solvation timescales of 130 ps (75%) and 2.35 ns (25%). As a parallel study, the minor-groove binding drug H258 is used to probe independently the dynamics of the minor groove of oligo1. The striking similarity of the observed timescales reported by both the probes provides direct evidence of minor-groove binding of DAPI in oligo1. In oligo2, the probe does not report any environmental relaxation in our experimental window. The absence of solvation, the fluorescence quenching due to an electron-transfer process (30 ps, in our resolution), and the presence of an  $\sim$ 150 ps component in the fluorescence lifetime of DAPI both in oligo2 and in bulk buffer have been correlated with the intercalative binding mode of the dye. The dynamics of DAPI in calf thymus DNA having a random sequence is similar to that of DNA in the minor groove. Our studies clearly explore the structure–dynamics correlation of the DAPI–DNA complex in the two distinct modes of interaction of DAPI with DNA.

**Acknowledgment.** D.B. thanks CSIR, India, for a fellowship. We thank DST for a financial grant (SR/FTP/PS-05/2004).

## References and Notes

- (1) Larsen, T. A.; Goodsell, D. S.; Cascio, D.; Grzeskowiak, K.; Dickerson, R. E. *J. Biomol. Struct. Dyn.* **1989**, *7*, 477–491.
- (2) Wilson, W. D.; Tanious, F. A.; Barton, H. J.; Strekowski, L.; Boykin, D. W. *J. Am. Chem. Soc.* **1989**, *111*, 5008–5010.
- (3) Kim, S. K.; Eriksson, S.; Kubista, M.; Norden, B. *J. Am. Chem. Soc.* **1993**, *115*, 3441–3447.
- (4) Vlieghe, D.; Sponer, J.; Meervelt, L. V. *Biochemistry* **1999**, *38*, 16443–16451.
- (5) Barcellona, M. L.; Cardiel, G.; Gratton, E. *Biochem. Biophys. Res. Commun.* **1990**, *170*, 270–280.
- (6) Wilson, W. D.; Tanious, F. A.; Barton, H. K.; Jones, R. L.; Fox, K.; Wydra, R. L.; Strekowski, L. *Biochemistry* **1990**, *29*, 8452–8461.
- (7) Jansen, K.; Norden, B.; Kubista, M. *J. Am. Chem. Soc.* **1993**, *115*, 10527–10530.
- (8) Trotta, E.; D'Ambrosio, E.; Ravagnan, G.; Paci, M. *Nucleic Acids Res.* **1995**, *23*, 1333–1340.
- (9) Trotta, E.; D'Ambrosio, E.; Ravagnan, G.; Paci, M. *J. Biol. Chem.* **1996**, *271*, 27608–27614.
- (10) Trotta, E.; Paci, M. *Nucleic Acids Res.* **1998**, *26*, 4706–4713.
- (11) Boger, D. L.; Fink, B. E.; Brunette, S. R.; Tse, W. C.; Hedrick, M. P. *J. Am. Chem. Soc.* **2001**, *123*, 5878–5891.
- (12) Colson, P.; Bailly, C.; Houssier, C. *Biophys. Chem.* **1996**, *58*, 125–140.
- (13) Eriksson, S.; Kim, S. K.; Kubista, M.; Norden, B. *Biochemistry* **1993**, *32*, 2987–2998.
- (14) Tanious, F. A.; Veal, J. M.; Buczak, H.; Ratmeyer, L. S.; Wilson, W. D. *Biochemistry* **1992**, *31*, 3103–3112.
- (15) Zou, S.; Baskin, J. S.; Zewail, A. H. *Proc. Natl. Acad. Sci. U.S.A.* **2002**, *99*, 9625–9630.
- (16) Pal, S. K.; Zhao, L.; Zewail, A. H. *Proc. Natl. Acad. Sci. U.S.A.* **2003**, *100*, 8113–8118.
- (17) Pal, S. K.; Zewail, A. H. *Chem. Rev.* **2004**, *104*, 2099–2123.
- (18) Bagchi, B. *Annu. Rep. Prog. Chem.* **2003**, *99*, 127–175.
- (19) Bandyopadhyay, S.; Chakraborty, S.; Balasubramanian, S.; Bagchi, B. *J. Am. Chem. Soc.* **2005**, *127*, 4071–4075.
- (20) Jordanides, X. J.; Lang, M. J.; Song, X.; Fleming, G. R. *J. Phys. Chem. B* **1999**, *103*, 7995–8005.
- (21) Brauns, E. B.; Madaras, M. L.; Coleman, R. S.; Murphy, C. J.; Berg, M. A. *J. Am. Chem. Soc.* **1999**, *121*, 11644–11649.
- (22) Brauns, E. B.; Madaras, M. L.; Coleman, R. S.; Murphy, C. J.; Berg, M. A. *Phys. Rev. Lett.* **2002**, *88*, 158101(1–4).
- (23) Sarkar, R.; Pal, S. K. *Biopolymers* **2006**, *83*, 675–686.
- (24) Shaw, A. K.; Pal, S. K. *J. Phys. Chem. B* **2007**, *111*, 4189–4199.
- (25) O'Connor, D. V.; Phillips, D. *Time Correlated Single Photon Counting*; Academic Press: London, 1984.
- (26) Jin, R.; Breslauer, K. J. *Proc. Natl. Acad. Sci. U.S.A.* **1988**, *85*, 8939–8942.
- (27) Pjura, P. E.; Grzeskowiak, K.; Dickerson, R. E. *J. Mol. Biol.* **1987**, *197*, 257–271.
- (28) Banerjee, D.; Pal, S. K. *Chem. Phys. Lett.* **2006**, *432*, 257–262.
- (29) Reha, D.; Kabelac, M.; Ryjacek, F.; Sponer, J.; Sponer, J. E.; Elstner, M.; Suhai, S.; Hobza, P. *J. Am. Chem. Soc.* **2002**, *124*, 3366–3376.

(30) Mazzini, A.; Cavatorta, P.; Iori, M.; Favilla, R.; Sartor, G. *Biophys. Chem.* **1992**, *42*, 101–109.

(31) Barcellona, M. L.; Gratton, E. *Biophys. Chem.* **1991**, *40*, 223–229.

(32) Haddox, R. M.; Finklea, H. O. *J. Phys. Chem. B* **2004**, *108*, 1694–1700.

(33) Concepcion, J. J.; Brennaman, M. K.; Deyton, J. R.; Lebedeva, N. V.; Forbes, M. D. E.; Papanikolas, J. M.; Meyer, T. J. *J. Am. Chem. Soc.* **2007**, *129*, 6968–6969.

(34) Shaw, A. K.; Pal, S. K. *J. Photochem. Photobiol. B: Biol.* **2007**, *86*, 199–206.

(35) Shieh, H.-S.; Berman, H. M.; Dabrow, M.; Neidle, S. *Nucleic Acids Res.* **1980**, *8*, 85–98.

(36) Pal, S.; Maiti, P. K.; Bagchi, B. *J. Chem. Phys.* **2006**, *125*, 234903(1-11).

(37) Furstenberg, A.; Julliard, M. D.; Deligeorgiev, T. G.; Gadjev, N. I.; Vasilev, A. A.; Vauthey, E. *J. Am. Chem. Soc.* **2006**, *128*, 7661–7669.